

# Velocity-Matched Distributed Photodetectors with p-i-n Photodiodes

M. S. Islam, T. Jung, S. Murthy, T. Itoh, M. C. Wu, D.L. Sivco<sup>†</sup>, and A.Y. Cho<sup>†</sup>

University of California, Los Angeles, Dept. of EE, 63128 Engineering IV, Box 951594, Los Angeles CA 90095-1594, USA. Tel: (310) 825-6859, Fax: (310) 794-5513, email: wu@ee.ucla.edu

<sup>†</sup>Lucent Technologies, Bell Laboratories, Murray Hill, NJ 07974, USA

## ABSTRACT

We report on the first demonstration of velocity-matched distributed p-i-n photodetectors. Record high linear DC photocurrent of 45 mA has been achieved without suffering from thermal damage, thanks to the superior power handling capability of p-i-n photodiodes. The frequency response is flat from 1 GHz to 35 GHz.

## I. INTRODUCTION

High power, high-speed photodetectors are a key component for microwave fiber optic links and optoelectronic generation of microwave and millimeter-waves [1]. High optical power can greatly enhance the link gain, signal-to-noise-ratio and the spur free dynamic range (SFDR) of externally modulated links. Several approaches have been proposed to increase the maximum linear photocurrent of high-speed photodetectors, including waveguide photodetectors with low confinement factors [2-4], traveling-wave photodetectors [5,6] and phototransistors [7], velocity-matched distributed photodetectors (VMDP) [8,9], and parallel fed VMDP [10]. Using the VMDP with metal-semiconductor-metal (MSM) photodiodes (PDs), we have achieved a saturation photocurrent of 33 mA at 1.55  $\mu\text{m}$  wavelength [8]. Bimberg *et al.* also reported on an MSM-based VMDP with a bandwidth above 78 GHz [9].

The maximum linear photocurrent in our previous MSM-VMDP is limited by the catastrophic damage caused by thermal runaway. p-i-n PDs have higher threshold for thermal runaway than MSM photodiodes. It was previously shown that MSM photodiodes fail at junction temperatures of  $\sim 700\text{K}$  [11], whereas p-i-n can stand junction temperatures above 900K [12]. This is primarily due to the larger barrier height for dark current in p-i-n photodiodes. Therefore, VMDPs with p-i-n photodiodes can achieve even higher photocurrent. Moreover, the uniform electric field distribution in p-i-n is also advantageous for linear operation under high power illumination. Moreover, the fabrication of high

bandwidth MSM photodiodes demands sophisticated sub micron e-beam writing and thin MSM fingers are vulnerable to failure caused by high photocurrents. Therefore, VMDP with p-i-n photodiodes are of great interest for high power photodetection.

In this paper, we report on the first demonstration of the VMDP with p-i-n photodiodes. Record-high linear photocurrent of 45mA has been achieved. No thermal runaway was observed for photocurrent above 55 mA. Our VMDP has a flat frequency response up to 35 GHz, though there is an initial drop at low frequency due to slow carrier diffusion. We have also found that the maximum linear photocurrent is dependent on the alignment of input optical fibers. The fiber position for maximum responsivity is different from that for maximum linear photocurrent. A unique technique has been developed to achieve the optimum fiber alignment.

## II. DESIGN AND FABRICATION

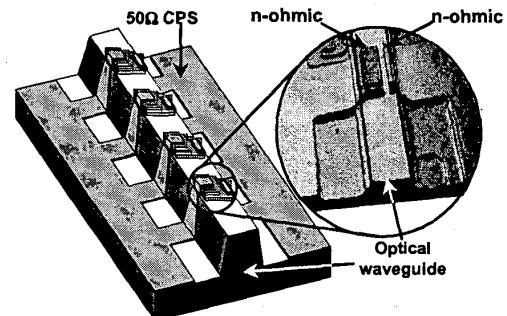


Fig. 1. Schematics of the VMDP with a close-up view of the active p-i-n photodiode region.

The schematic structure of the VMDP is illustrated in Fig. 1. A linear array of p-i-n photodiodes is periodically distributed on top of a passive optical waveguide. Optical signal is evanescently coupled from the passive waveguide to the active p-i-n PDs. Photocurrents generated from the individual photodiodes are added in phase through a 50 $\Omega$  coplanar strips (CPS) microwave

transmission line that is velocity-matched to the optical waveguide. The photodiodes are kept below saturation by coupling only a small fraction of optical power to each photodiode.

The active p-i-n PDs consist of a 0.25- $\mu\text{m}$ -thick InGaAs absorption layer and two InGaAlAs ohmic contact layers. One of the main tradeoffs in the design of p-i-n VMDP is the placement of ohmic contacts. Fig. 2 shows three different contact schemes: (a) parallel contacts on a continuous waveguide, (b) tandem contacts on a continuous waveguide, and (c) parallel contacts with lower contact outside the waveguide. The contact area for each photodiode is  $20 \times 2.5 \mu\text{m}^2$ . In our device, the p-ohmic contact is the lower contact, which is close to the core of the passive waveguide. We experimentally investigated the performances of the VMDPs with different contact schemes. Our experimental results show that VMDPs with Scheme (a) contacts have the best performance: they have the lowest loss and more uniform photocurrent distribution along the waveguide. The spacing between the n and p contacts is  $2 \mu\text{m}$ .

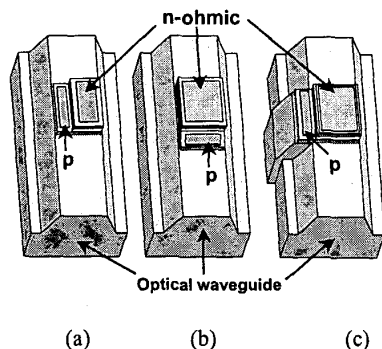


Fig. 2. Schematics of three different contact schemes. (a) parallel on continuous waveguide (b) tandem on continuous waveguide (c) parallel contacts with lower contact outside the waveguide.

A wide horizontally multimode optical waveguide with continuous transitions between passive waveguide and active PD is employed to reduce interface losses. Since the microwave velocity can only be matched to the group velocity of one optical mode, there is some inherent velocity mismatch in multimode devices. However, the mismatch is small ( $< 10\%$ ) and the bandwidth limit due to velocity mismatch is greater than 150 GHz, which is higher than the transit time-limited bandwidth of our current device. Moreover, our BPM simulation shows that more than 97% of the input power is coupled to the fundamental mode during propagation.

### III. MEASUREMENTS AND DISCUSSION

The DC responsivity is 0.42 A/W at 1 V bias (without AR coating). This responsivity can be further improved by employing airbridges to connect photodiodes with the microwave transmission line, which prevent direct metal deposition on the sidewalls of the waveguide. The reverse bias breakdown is  $\sim 1.5\text{V}$ . The low breakdown is caused by the diffusion of p-type dopants from the lower contact layers into the InGaAs absorbing layer during the epitaxial growth. The microwave characteristics of the VMDP is measured by HP 8510C network analyzer. The measured characteristic impedance matches very well to  $50 \Omega$  (within 3%) for a broad frequency range.

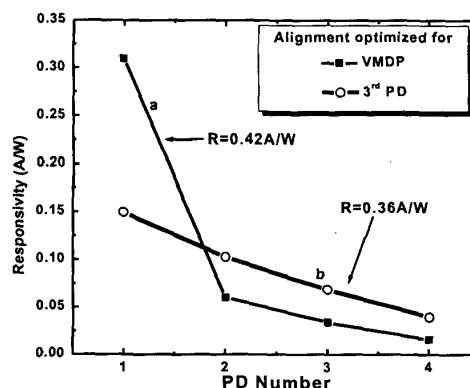


Fig. 3. Measured responsivity of each PDs in the split contact VMDP for focusing the input power to the whole structure and for focusing to the 3<sup>rd</sup> photodiode.

To characterize the distribution of photocurrents within the VMDP, we have fabricated VMDPs with separate contacts for each photodiodes. We found the photocurrent distribution is sensitive to the alignment of input optical fibers. The measurement results are shown in Fig. 3. When the fiber is positioned to optimize the overall responsivity of the VMDP (0.42 A/W), the photocurrent distribution has a very steep decay (Curve (a) of Fig. 3). The first photodiode contributed 73.8% of the overall photocurrent. The maximum linear photocurrent is 22 mA. If the fiber is positioned to optimize the response of the second photodiode instead of the entire VMDP, more uniform distribution of photocurrent is obtained. The responsivity of the overall VMDP decreased slightly to 0.39 A/W, however, the maximum linear photocurrent increased to 35 mA. This is because more photodiodes are contributing to the total photocurrent when the first photodiode reaches saturation. If we move the fiber again to optimize

response of the *third* photodiode, the maximum linear photocurrent of the VMDP is increased further to 45.5 mA. The overall responsivity became 0.36 A/W. The distribution of photocurrent under this coupling condition is shown in Fig. 3 (line b).

The explanation for the above observation is as follows. Because the first photodiodes is located very close to the facet (100  $\mu\text{m}$  away), the optical field coupled into VMDP has not reached the steady state distribution yet. The transient field can be directly coupled into the photodiodes, resulting in higher photocurrents in the first photodiode. Therefore, when we align the fiber by maximizing the overall response of the VMDP, the fiberto-waveguide coupling is actually not optimized. Though the absorption of the transient field helps increase the overall quantum efficiency, the extra photocurrent concentrates in the first photodiode and causes it to saturate at lower overall photocurrent. The photocurrents of the photodiodes farther away from the input facet are less influenced by the transient field and, therefore, are better monitors for the fiber alignment.

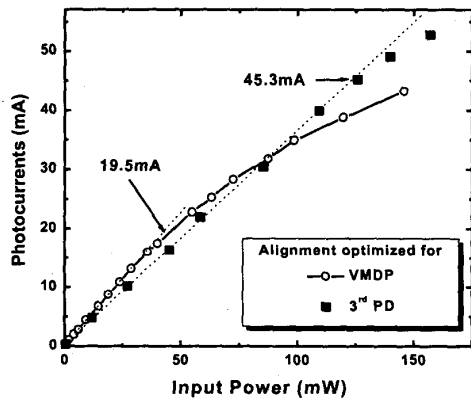


Fig. 4. Measured DC linear photocurrents for two different input fiber positions. The linear current improve greatly when the input power is optimized to a distant photodiode.

This above technique can be used to improve the maximum linear photocurrent of an identical VMDP with the same device geometry but without split contacts. The displacement of the fiber between the optimum responsivity and the maximum photocurrent of a distant (e.g., the 3<sup>rd</sup>) PD is very reproducible. Therefore, we can calibrate the displacement ( $\Delta X$ ,  $\Delta Y$ , and  $\Delta Z$ ) first using a split-contact VMDP. To align the fiber to a regular VMDP without split contact, it is first aligned to maximize the overall responsivity. This leads to concentration of photocurrent in first PD. We then move the fiber by  $\Delta X$ ,  $\Delta Y$ , and  $\Delta Z$  using a piezo-controlled micrometer. This reduces the

photocurrent in the first PD and increases the contribution of diodes further down along the array. In all cases, the results are within 5% of that of that obtained from the split-contact test structure. Fig. 4 shows the photocurrents for both optimized coupling to the whole device and for focusing the input power to the 3<sup>rd</sup> PD using this technique. We achieved more than 45mA of linear photocurrent. To our knowledge, this is the highest linear DC photocurrent reported in high-frequency photodetectors.

Our finding also suggests new VMDP structures with built-in monitor for optimum fiber alignment. In addition to the regular array of PDs of the VMDP, we can add an additional monitoring photodiode in the middle of the waveguide (e.g., between the 4<sup>th</sup> and the 5<sup>th</sup> PDs). By optimizing the photocurrent of the monitoring PD, we can achieve high linear photocurrent. Alternatively, we can also employ a much longer passive waveguide to reduce the influence of transient field on the photocurrent of the first PD.

In contrast to the MSM VMDP we reported previously [8], the p-i-n VMDP does not fail at the maximum linear photocurrent. In fact, our device survives at photocurrent as high as 55 mA. If we continue to increase the photocurrent, eventually the facet of the optical waveguide is damaged at 200 mW. Even under this circumstance, the active PDs of the p-i-n VMDP remains alive. In fact, we can reverse the VMDP and couple light in from the undamaged facet, and obtain the same level of maximum linear photocurrent as before.

The responsivity of the VMDP can be improved by employing antireflection (AR) coating. The fiber coupling efficiency can be improved by integrating a spotsize converter for better mode-matching with fiber. Coupling efficiency as high as 90% has been reported [13]. With both AR coating and spot size converter, the responsivity can potentially be increased to 0.9 A/W. The optical power damaging level will also be increased.

We used both frequency and time domain measurements to characterize the AC response of the VMDP. The frequency domain measurement was performed by optical heterodyning method using two external cavity tunable lasers at 1550 nm. The optical signals are combined by a 3dB coupler, and coupled to the VMDP through a fiber pickup head. The output is collected by a 50-GHz probe and monitored by an RF power meter. The calibrated frequency response of the VMDP is shown in Fig. 5. The AC response has a quick rolloff at low frequencies (below 1 GHz) and then remains almost flat. The initial roll off at low frequency is due to the slow carrier diffusion in the active region, which is caused by unintentional migration of p-dopants (Be)

during epitaxial growth. Excluding the low frequency roll-off, the 3-dB frequency is 35GHz.

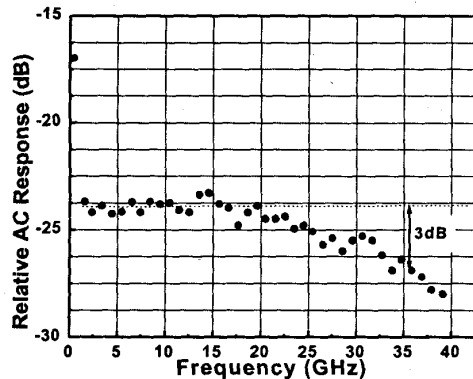


Fig. 5. Measured frequency response of the  $p-i-n$  VMDP with optical heterodyning. Except a sharp rolloff below 1GHz, the device has a 3-dB bandwidth  $>35$  GHz.

We have also measured the time domain pulse response of the VMDP. Short laser pulses with a FWHM pulse width of 1ps, a repetition rate of 25 MHz, and a center wavelength of 1550 nm are employed for the measurement. A VMDP with 8 PDs (each PD has an area of  $45\mu\text{m}^2$ ) was illuminated with an average photocurrent of 0.1mA and the resulting pulses were observed on a 50GHz sampling scope. Fig. 6 shows the measured results. The measured FWHM width is 13ps after deconvolving the response of the 50GHz scope. The measured results also include the losses of the microwave components. In addition to the short pulse, there is a long tail due to dopant migration in to the active region of the photodiode that contributes to slow carrier diffusion. This agrees well with the frequency domain measurement.

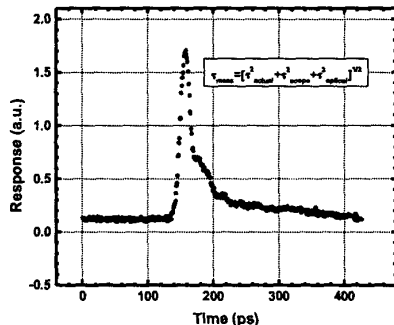


Fig. 6. Measured pulse response of the VMDP. The FWHM is 18ps without including the correction factors. The long tail is caused by the slow carrier diffusion in the dope active region.

A new epi-layer with a setback region is currently being developed to eliminate the low frequency roll off and increase the breakdown voltage. Another issue of our current devices is the

high contact resistance of the lower Ohmic contact, which results in low RC-limited bandwidth. Our current epitaxial layer structure does not have an effective stop etch layer before the lower Ohmic contact layer. As a result, the contact is actually formed on the InGaAlAs layer with low doping concentration. In the new epitaxial layer design, we have also inserted a stop etch layer to improve the contact resistance. The new device should exhibit higher frequency response.

#### IV. CONCLUSION

We have successfully demonstrated a velocity matched distributed photodetector with  $p-i-n$  photodiodes. A high linear DC photocurrent of 45 mA has been achieved. In order to increase the DC linear photocurrents a novel alignment technique is demonstrated. The VMDP has a flat frequency response from 1 to 35 GHz. A low frequency roll off due to slow carrier diffusion is also observed. We are now in the process of designing a new epitaxial structure to eliminate the long diffusion tail and improve the contact resistance.

#### V. ACKNOWLEDGEMENT

The authors would like to acknowledge Allan Hui, Wibool Piyawattanametha and Sagi Mathai of UCLA for their help. This project was supported by ONR MURI on RF photonics, and UC MICRO.

#### REFERENCE:

- [1] C.H. Cox, III *et al.*, "An analytic and experimental comparison of direct and external modulation in analog fiberoptic links," *IEEE MTT*, vol. 38, no. 5, p 501, May 1991.
- [2] D.C. Scott *et al.*, "Measurement of IP3 in  $p-i-n$  photodetectors and proposed performance requirements for RF fiber-optic links," *IEEE Photon. Technol. Lett.*, vol. 12, no 4, p 422, April, 2000.
- [3] S. Jasmin *et al.*, "Diluted and distributed-absorption microwave waveguide photodiodes for high efficiency and high power," *IEEE MTT*, vol.45, no.8, p.1337, 1997.
- [4] A.R. Williams *et al.*, "InGaAs/InP waveguide photodetector with high saturation intensity," *El. Letts*, vol.28, no.24, p.2258, 1992.
- [5] K.S. Giboney, M.J.W. Rodwell, J.E. Bowers, "Traveling-wave photodetector theory," *IEEE MTT*, vol.45, no.8, p.1310, 1997.
- [6] D. Jäger *et al.*, "Distributed velocity-matched 1.55 $\mu\text{m}$  InP traveling-wave photodetectors for generation of high millimeterwave signal power," *IEEE MTT-S Digest*, p1233, 1998.
- [7] D.C. Scott *et al.*, "High-power high-frequency travelingwave heterojunction phototransistors integrated polyimide waveguide" *IEEE Micro. and Guided Wave Lett.*, vol.8, no.8, p. 284, Aug. 1998.
- [8] M.S. Islam *et al.*, "High power distributed balanced photodetectors with high linearity", *International Microwave Photonics Conf.*, Melbourne, Australia, 16-19 Nov, 1999.
- [9] Bimberg, *et al.*, "78 GHz distributed InGaAs MSM", *Electronics Letters*, vol.34, no.23, IEE, p.2241-3, 1998.
- [10] S. Murthy *et al.*, "A novel monolithic distributed traveling wave photodetector parallel opt. feed," *IEEE Phot. Tech. Lett.*, June, 2000.
- [11] A. Nespola *et al.*, "Failure analysis of travelling wave MSM distributed photodetectors," *IEDM*, San Francisco, CA, USA, 1998.
- [12] K.J. Williams and R.D. Esman, "Design considerations of high current photodetectors," *IEEE JLT*, vol.17, no.8, p.1443, Aug. 1999.
- [13] A. Umbach *et al.*, "Ultrafast, high-power 1.55 $\mu\text{m}$  side-illuminated photodetector with integrated spot size converter," *OFC 2000*, Baltimore, MD, March 7-10, 2000.